Journal of African Earth Sciences 168 (2020) 103867

Contents lists available at ScienceDirect

Journal of African Earth Sciences

journal homepage: www.elsevier.com/locate/jafrearsci

Gravity aspects from recent Earth gravity model EIGEN 6C4 for geoscience and archaeology in Sahara, Egypt

Jaroslav Klokočník[a], Václav Cílek[b], Jan Kostelecký[c,d], Aleš Bezděk[a,e,*]

[a] Astronomical Institute, Czech Academy of Sciences, CZ 251 65, Ondřejov, Fričova 298, Czech Republic
[b] Geological Institute, Czech Academy of Sciences, CZ 165 00, Praha 6, Rozvojová 269, Czech Republic
[c] Research Institute of Geodesy, Topography and Cartography, CZ 250 66, Zdiby 98, Czech Republic
[d] Faculty of Mining and Geology, VSB-TU Ostrava, CZ 708 33, Ostrava, Czech Republic
[e] Faculty of Civil Engineering, Czech Technical Univeristy in Prague, CZ 166 29, Praha 6, Czech Republic

ARTICLE INFO

Keywords:
Eastern Sahara/Great sand sea
Paleolakes
Holocene occupations
EIGEN 6C4 gravity Model
Gravity aspects
Impact crater
Libyan desert glass

ABSTRACT

A new method to detect paleolakes via their gravity signal is presented (here with implications for geoscience and archaeology). The gravity aspects or descriptors (gravity anomalies/disturbances, second radial derivatives, strike angles and virtual deformations) were applied. They were computed from the gravity field model EIGEN 6C4 (European Improved Gravity model of the Earth by New techniques). The model consists of the best now available satellite and terrestrial data, including gradiometry from the GOCE (Gravity field and steady-state Ocean Circulation Explorer) satellite mission. EIGEN 6C4 has the ground resolution ~10 km. From archaeological sources, the positions of archaeological sites of the Holocene occupations between 8500 and 5300 BCE (8.5–5.3 ky BC) in the Eastern Sahara, Western Desert, Egypt were taken. They were correlated with the features found from the gravity data; the correlation is good, assuming that the sites were mostly at paleolake borders or at rivers. Based on this finding, we suggest position, extent and shape of paleolake(s). We also reconsider the origin of Libyan Desert glass in the Great Sand Sea and support hypothesis about an older impact structure created there, repeatedly filled by water, which might be a part of some of the possible paleolake(s).

1. Introduction

The aim of this work is mainly to correlate the gravity aspects (descriptors), defined in Kalvoda et al. (2013) or Klokočník et al. (2017b), derived from a recent gravity field model, with archaeological sites. These were climate-controlled occupations in the Eastern Sahara (Fig. 1a–b, 2a-d) during the main humid phases of the Holocene before general dessication (drying up) approx. 2,5–2,2 ky BC. We propose the existence of a large lacustrine possibly Miocene (23-5 My) or older basin that was later due to the preferential wind erosion of soft sediments partly exhumed in Quaternary (2,7 My) and maybe repeatedly functioned as shallow water body. Furthermore we speculate about the possible impact origin of this basin or its part.

Each density variation under the surface generates a gravity variation, more generally an anomalous gravity signal (a change in all the gravity aspects). For example, deficiency of masses or a lower density material results in a negative gravity anomaly. We are able to detect paleolakes (Klokočník et al., 2017a, 2018) according to their specific gravity signal in all the gravity aspects, not only by the gravity anomalies, see section *Notes on theory;* e.g., by negative gravity anomalies Δg, negative values of the second derivative of the disturbing potential in the radial direction T_{zz} or by compression in the virtual deformations *vd* or by places with one-way oriented ("combed") vectors of the strike angles θ. All these gravity aspects should be treated together, not separately, to provide a successful and most complete result. Today's deeper or wider river valleys are indicated by the same way as those hidden under the sand layers, as we can see in Fig. 3a–e for some parts of the Nile river, at Fayum, significantly in the Red Sea and elsewhere. When water disappears and is replaced by sand, the density contrast with respect to surrounding rocks becomes lower, but still exists, and this is what we can detect (if it is sufficiently large and strong, see more about resolution and precision in section about *Data*). What then remains are conspicuous negative Δg and T_{zz} and specific values of the other gravity aspects that we can see for example in the south and west direction from Kharga or along the Libyan-Egyptian border in the Great Sand Sea (GSS, Bahr al-Raml). These signals are preserved under the sand layers for a long time (but not forever; endogenous and exogenous forces are transporting masses from place to

* Corresponding author. Astronomical Institute, Czech Academy of Sciences, CZ 251 65, Ondřejov, Fričova 298, Czech Republic.
E-mail addresses: jklokocn@asu.cas.cz (J. Klokočník), cilek@gli.cas.cz (V. Cílek), kost@fsv.cvut.cz (J. Kostelecký), bezdek@asu.cas.cz (A. Bezděk).

https://doi.org/10.1016/j.jafrearsci.2020.103867
Received 17 February 2020; Received in revised form 27 April 2020; Accepted 27 April 2020
Available online 11 May 2020
1464-343X/

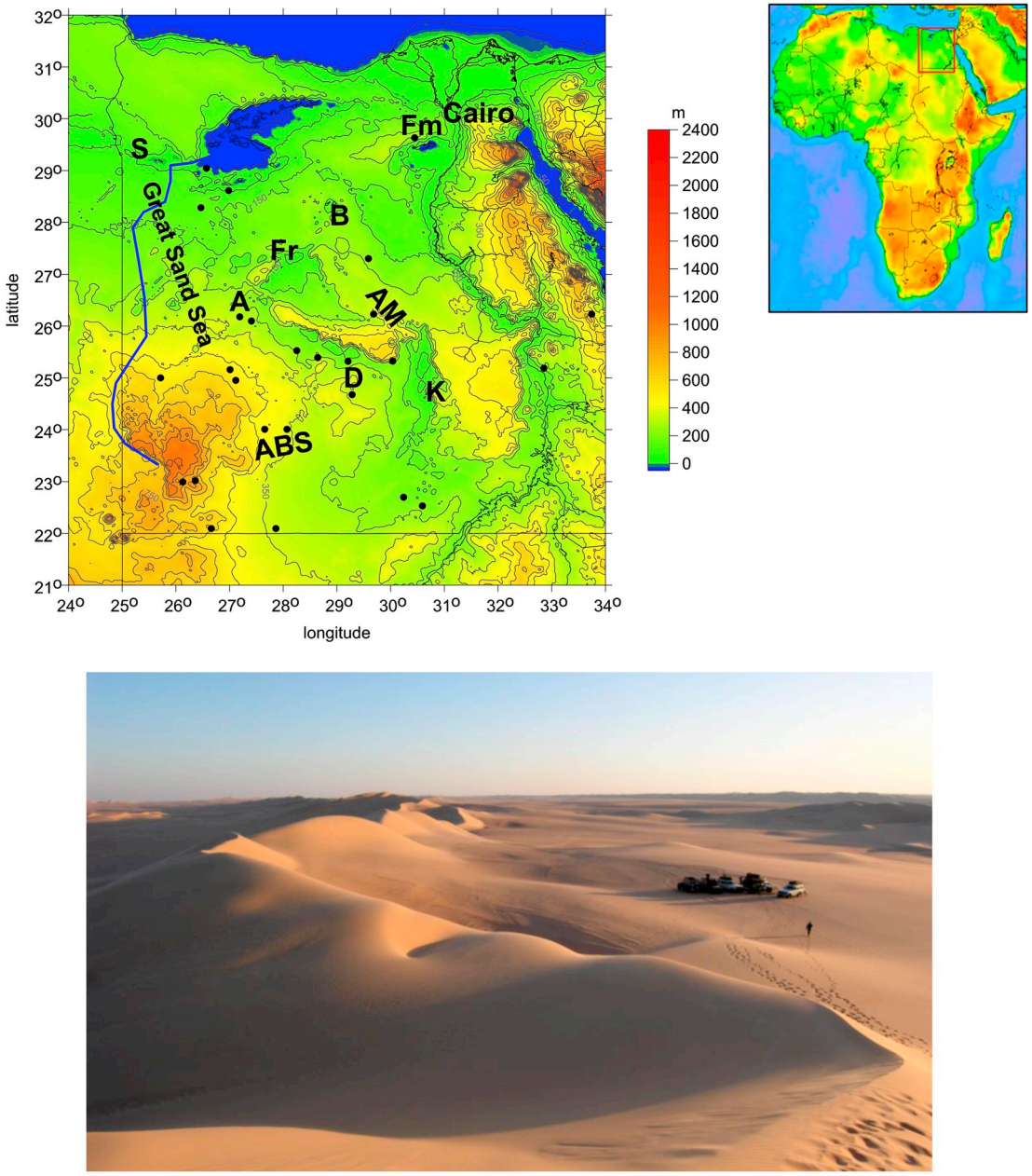

Fig. 1. a Surface topography of Egypt (heights above sea level in meters) from ETOPO 1. Blue colour does not inevitably mean water, but the fact that the terrain is below the present sea level (e.g. the depression at Siwa, NW). The curve in south-north direction (mostly along the Egyptian-Libyan border, where GSS is located) shows where the topographic and the gravity anomaly profiles (shown in Fig. 6 below) are passing. Our localities of interest: GSS Great Sand Sea, A Abu Minqar, B Bahariya, D Dakhla, Fr Farafra, Fm Fayum, K Kharga, AM Abu Muhariq Plateau, ABS Abu Ballas Scarp-land (Eastpans, Mudpans, Westpans), GK Gilf Kebir, S Siwa. Inlet: a digital elevation map of Africa showing the area of our study. **b** Characteristic view of the Great Sand Sea (GSS) consists of almost parallel long dune ridges. © V. Cílek 2008. (For interpretation of the references to colour in this figure legend, the reader is referred to the Web version of this article.)

place thus changing the local gravity field, too).

2. Notes to theory

We shortly outline theoretical preliminaries being aware that reader has probably another specialisation than the gravity field studies. But some basic information ("what is what") is inevitable. We just repeat what we have published elsewhere (for the full theory with examples see our book Klokočník et al., 2017b).

The core of our method is in the use of various gravitational aspects or descriptors (functions of the disturbing gravitational potential represented by a gravity field model), namely the gravity anomalies or disturbances Δg, the components of the Marussi tensor $\mathbf{\Gamma}$ of the disturbing potential, namely of the second radial derivatives T_{ij}, the gravity invariants I_1 and I_2, their specific ratio I, the strike angle θ and the virtual deformations *vd*. Each such *gravity aspect* tells its own "story" about the causative body (density variations) under the surface; the traditional gravity anomalies are not sufficient.

The theory underlying our methodology was transformed mainly from Pedersen and Rasmussen (1990) and Beiki and Pedersen (2010). A new (our own) part of the theory comes from Kalvoda et al. (2013); a complete review of the theory needed to understand this paper is in Klokočník et al. (2014, 2016, 2017a, b). We understand that reader may need more explanation about theory here, but we cannot repeat all due to selfplagiarism and length of the manuscript. Only shortly we recall *Theory* in the notes in the next few paragraphs.

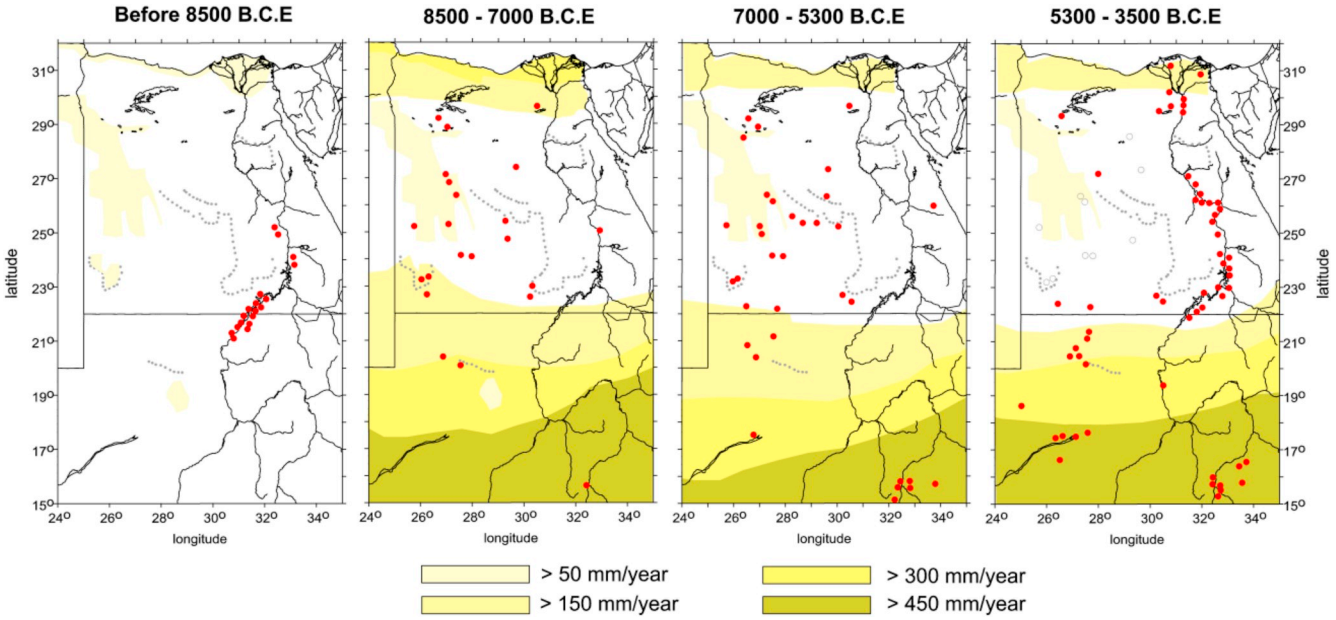

Fig. 2. a-d These important figures show the archaeological input data to our analyses: the climate-controlled occupation in the Eastern Sahara during the main phases of the Holocene. Based on Fig. 3 a-d in Kuper and Kroepelin (2006). With the abrupt arrival of monsoon rains at 8500 B.C.E. (=8.5 ky BC), the hyper-arid desert on west was replaced by savannah-like environments, while the Nile valley was too moist. After 5300 BCE, a dessication of the Egyptian Sahara began again. Here we correlate Fig. 3 b and *c* (8.5–5.3 ky BC), showing maximum of occupation west of Nile (from Kuper and Kroepelin, 2006) with the gravity aspects computed from the EIGEN 6C4 model to locate possible paleolake(s) – see the main text.

The Marussi tensor provides more complex information than the gravity anomalies (or disturbances) Δg only; T_{zz} informs about the target body location, the other components T_{ij} of $\mathbf{\Gamma}$ refer to the orientation and shape of the causative density anomalies. The components T_{ij} provide sharpening of the anomalies and enhancements of the high frequency content without changes in the location or shapes of the anomalies (e.g., Saad, 2006).

The invariants can be looked upon as non-linear filters enhancing the sources having big volumes; they discriminate major density anomalies into separate units. The specific ratio I (sometimes called "2D indicator") of I_1 and I_2 can indicate two-dimensionality of the causative body (e.g., Pedersen and Rasmussen, 1990, p. 1559). Condition $I = 0$ is necessary but not a sufficient condition for two-dimensionality.

The strike angle θ shows the main direction of $\mathbf{\Gamma}$. This may be an important direction for the underground object. When $I = 0$, the values of θ may indicate a dominant 2D ("flat") structure. It can be geophysically significant (related to oil&gas deposits, water or ground water, rivers, paleolakes, impact craters…).

The virtual deformation *vd* characterizes the "tensions" (compression or dilatation) generated by the causative body. We can understand *vd* as a principle axis transformation from the horizontal gradients of the deflection of vertical. The *vd* are *g*eometrically expressed by dilatation or compression, the dilatations indicate uplifted regions at the geoid, whose mass has a tendency to disintegration (owing or according to the pattern of values of the gravitational potential). The virtual compressions indicate lowered zones at the geoid. Natural processes, which are the cause of these states of the near-surface part of the geoid, are very diverse as a consequence of regionally heterogeneous integration of morpho-tectonic and erosion-denudation processes.

The concept of gravity aspects (descriptors) is relatively new and not too much known and used among geoscientists yet; but first applications of the aspects, for example of the virtual deformations, have already appeared (e.g. in Eppelbaum, 2017; Eppelbaum et al., 2017 for tectonic studies).

3. Data

The information about the gravity data, topography data, and archaeological data, which all together create an input to our analyses, is presented now.

The *gravity data* can be represented in various ways; for us, for the theory used and software developed, they are represented by a model of gravity/gravitational field of the Earth always expressed in terms of harmonic geopotential coefficients (also known as Stokes parameters). They were determined from various satellite and terrestrial data, to a certain maximum degree and order of spherical harmonic expansion (dictating consequently the ground resolution of the gravity field model).

The EIGEN 6C4 (*E*uropean *I*mproved *G*ravity model of the *E*arth by *N*ew techniques, Foerste et al., 2014) is a global combined, comprehensive and detailed gravity field model including gradiometry data from the whole GOCE mission (*G*ravity field and steady-state *O*cean *C*irculation *E*xplorer, ESA). The important fact is that EIGEN 6C4 is a better and higher resolution gravity model in a comparison with all its predecessors. Its worldwide resolution is 5x5 arcmin, which is about 10 km on the ground and its precision expressed as a typical standard deviation in the gravity anomalies is 10 mGal (Foerste, priv. commun.). The quality of EIGEN 6C4 is not expressed only by a resolution and precision, but also by a global and nearly regular coverage (excluding small polar gaps) by five year GOCE gradiometry data from ESA. In this study, we make use of EIGEN 6C4.

All the gravity aspects (Klokočník et al., 2017b) are computed from the selected gravity field model by software developed by (Bucha and Janák, 2013 and references therein) and by our own independent software (internal technical reports), with a special emphasis on numerical stability of the higher derivatives (it was not a trivial item, but will not be discussed here).

We emphasize that the input data to our computations are always and only the harmonic geopotential coefficients of a global gravity field model. We can not use for example the measured regional/local gravity anomalies or Marussi tensor components from gravimeters or gradiometers. It is also the case of Abd-Elmotaal et al. (2018) gravity

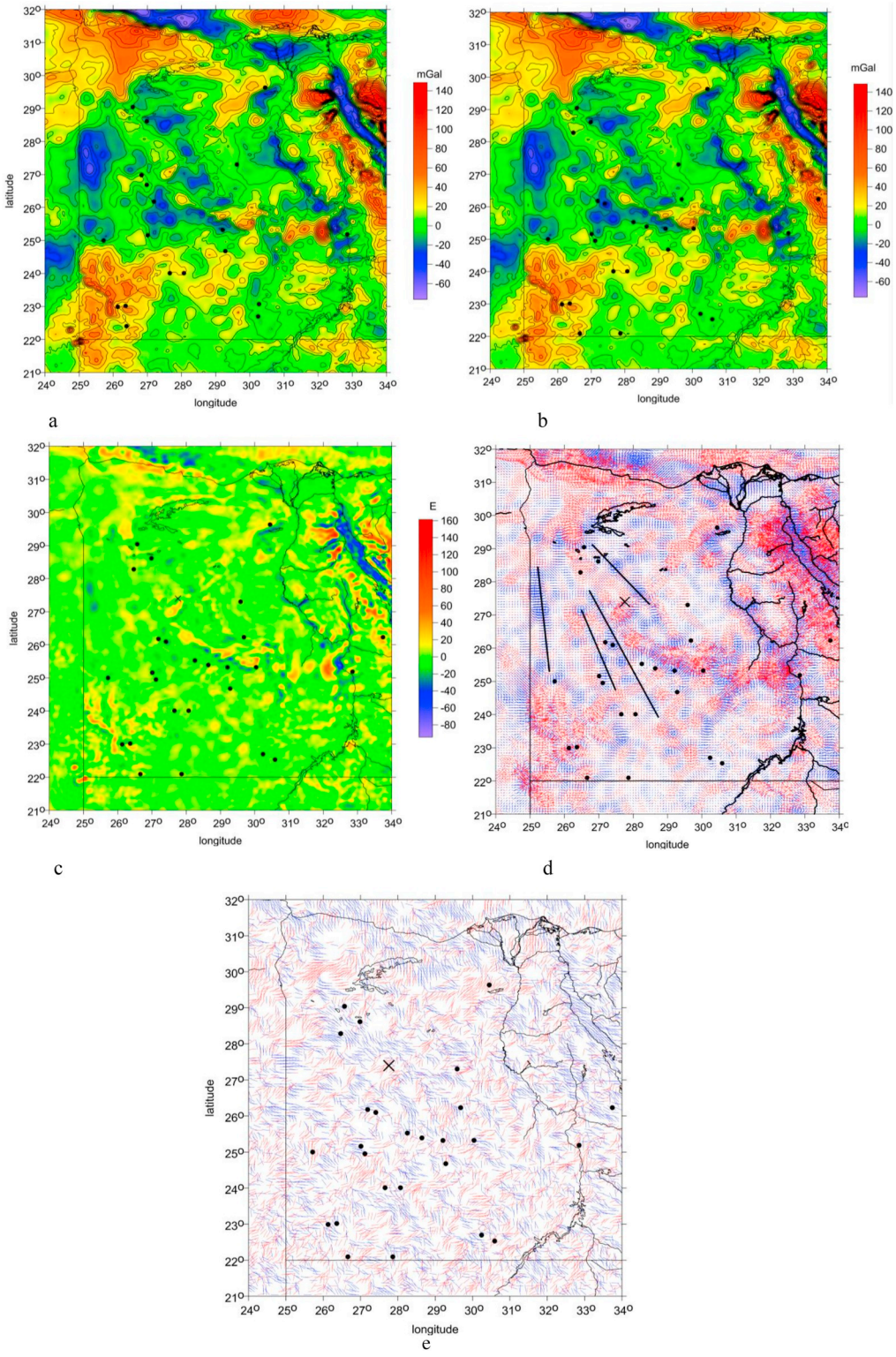

Fig. 3. a,b Gravity disturbances Δg [mGal] with contour lines using EIGEN 6C4 superposed over Fig. 3b for the period 8.5–5.3 ky BC and *3c* for the period 7.0–5.3 ky BC, both from Kuper and Kroepelin (2006), now black dots. Note *different black dots* in these figures; it is so because these two figures are valid for two different time periods. However, they are rather similar; therefore, for the further figures, we have chosen only the period 7.0–5.3 ky BC, because it contains more data (more black dots). Blue colour does not mean water but negative anomaly, in turn a potential place for a paleolake (in the area of GSS). A part of settlements (south and south-west of Egypt) outside lowlands (like Gilf Kebir and Abu Ballas Scarp-land from Gilf Kebir to Dakhla) can not be correlated with paleolakes, but with now existing wadis remaining after some rivers in this hilly area. **c, d** The second radial derivative T_{zz} [E] and the virtual deformations (*vd*) in the same area and with EIGEN 6C4; red for dilatation, blue for compression; superposition now only for Fig. 3c (7.0–5.3 ky BC) from Kuper and Kroepelin (2006). The cross is for the cave El Obeyid at Faráfra oasis (geodetic latitude 27°23.745′N, longitude 27°45.469′E), see a photo below. About the black radials see more in the text. **e** The strike angles θ [deg] (for the ratio $I < 0.3$ to emphasize roughly flat underground zones) with EIGEN 6C4 (expressed in degrees with respect to the local meridian, in red colour to the east and in blue to the west of the meridian); the important fact is that in some zones these angles are locally "combed" into one direction; more explanation is in the text; superposition only for Fig. 3c (7.0–5.3 ky BC) from Kuper and Kroepelin (2006). . (For interpretation of the references to colour in this figure legend, the reader is referred to the Web version of this article.)

anomaly database for Egypt and the new work by Sobh et al. (2019). For a regional gravity field model for Egypt, they combined satellite and ground-based data (including those derived from GOCE). We refer to their Fig. 1 with terrestrial data coverage for Egypt. It should be similar to that of EIGEN 6C4 which is based on an older EGM 2008 US database (Pavlis et al., 2012) with some additional data (see more in Foerste et al., 2014). The conclusion for us is that our study area in west Egypt is well covered although not everywhere on 100%.

Topography data. ETOPO 1 (Fig. 1a for Egypt) is a part of the global 1-arcmin (cell size) relief model of the Earth surface that integrates land topography and ocean bathymetry from huge number of satellite measurements (Amante and Eakins, 2009). Its precision is about 10–15 m in heights (but not everywhere). For us, it is a subsidiary input data set. We know about other satellite topography data sets, we tested them and compared them to ETOPO 1 over Sahara, but we do not use them here. The stated precision may be only an internal precision not the actual external accuracy.

Archaeological input data. Kuper and Kroepelin (2006) published the

data about occupation of the area; they are very important for us as the input data. They studied, among others, climate-controlled Holocene occupation in the Sahara since the onset of humid conditions about 11 ky BC. We make use of their results presented here – in a modified version they are reviewed as Fig. 2a–d. Without this input, our paper would not exist.

The river and paleolake systems (not only at today's GSS) would be crucial for life and migration. But river corridors and wet areas might exist here much earlier and only might be recently re-opened; a novel palaeohydrological and hydraulic modelling approach tested the hypothesis that under wetter climates 100–130 ky ago major river systems ran north across the Sahara to the Mediterranean, creating viable migration routes, including rivers flowing from south to north in the area of today's GSS (e.g. Coulthard et al., 2013).

The vital part played by river valleys and lakes or inner seas in human prehistory is evident. “The riverine environments offered not only attractive living space but also the logical pathways to new lands…” wrote Burroughs (2005). The relative climate stability that was the hallmark of the Holocene, provided evident benefit of riverside/lakes sites stability.

Gehlen et al. (2002) studied the Holocene occupation of the Eastern Sahara. Their results are accounted here to locate possible paleolakes and paleoriver systems; we refer to their Fig. 1. Paleolakes and implications to groundwater accumulation in Eastern Sahara and namely in GSS were predicted already by Farouk El-Baz (1998). Here we work with probably most modern results – with the data about Holocene occupations gathered by Kuper and Kroepelin (2006), their Fig. 3 a-d, here transformed to Fig. 2a–d.

4. Geological-archaeological results and their interpretation

In Fig. 1a we show a detailed surface topography by contour lines derived from the digital elevation model ETOPO 1 together with a location map. The area of GSS looks like a huge flat plate (ignoring the dunes), slightly inclined from the south (north of Gilf Kebir plateau about 1000 m above sea level, see the symbol GK in Fig. 1a) to the north (near Siwa oasis which is below today's sea level, S in Fig. 1a) into the Mediterranean sea. It is about 600 km long from south to north and up to about 300 km wide (Fig. 1b). Rivers flew here in the Holocene from the south to the north. GSS does not exhibit any considerable (high, huge) topographic features. But the gravity aspects here are far from to be “flat” – see our results in Fig. 3a–e. Such a “rich”, variable gravity signal is hidden under the sand, having pronounced depressions in Δg, T_{zz} or in vd.

The gravity disturbances Δg [mGal] with contour lines, using the full gravity model EIGEN 6C4, are shown in Fig. 3 a-b. They are superposed over Fig. 3 b and *c* (for the periods 8.5–5.3 ky BC) from Kuper and Kroepelin (2006), showing maximum of occupation (after and before dry periods in this area). The difference between Fig. 3b and *c* in (Kuper and Kroepelin, 2006) is small as for the occupation sites, so we present the other gravity aspects only with superposition to Fig. 3c of (Kuper and Kroepelin, 2006), i.e. for the period 7.0–5.3 ky BC (with more “data dots”). The second radial derivatives T_{zz}[E] are in our Fig. 3c, the virtual deformations (vd [−]) in Fig. 3d and the strike angles (θ [deg]) in Fig. 3e.

We focus on the area west of the Nile river, on GSS. With Fig. 3a and b we can locate 24 dots for the occupation sites for the period 7.0–5.3ky BC, 20 of them in a low-land, probably close to hypothetical paleolakes (at supposed shores). Only 4 dots are in high-lands (hills at Gilf Kebir, north and east of it, at rivers, now wadis). A correlation between the gravity anomalies and the occupation sites is evident.

T_{zz} (Fig. 3c) indicates a gradient in Δg, so for example in the west part of GSS (along the border with Libya), we can expect a deeper slope in the paleolake. Note also large changes in the T_{zz} values in Fayum, at some part of the Nile, Dakhla, and of course inside the Red Sea.

Note on precision: we work with the gravity data ground resolution about 10 km, with occupation sites locations taken from *Fig. 3 a-d* in Kuper and Kroepelin (2006), which cannot also be too much precise and therefore, we have to reconcile to only an approximate estimate on the paleolake positions, also with something like 10 km (an intuitive estimate or speculation only).

How deep and large might be that valley in the GSS and elsewhere? First the depth. We will use relationship between the gravity anomaly (free air anomaly) Δg and the relevant height difference Δh (e.g., Pick et al., 1973):

$$\Delta g_{\,[\mathrm{mGal}]} = (0.3086–0.0419\ \rho)\ \Delta h_{[\mathrm{m}]}. \quad (1)$$

We take the densities of dry sand ρ = 1.4–1.7 g/cm^3 and that of typical non-volcanic rocks ρ = 2.6–2.7 [g/cm^3]. We will need to know the difference $\Delta\rho$ so we consider $\Delta\rho \approx 1$ g/cm^3. From eq (1) we derived:

$$\Delta h_{[\mathrm{m}]} = \Delta g\ /\ 0.2667 = 3.75\ \Delta g_{\,[\mathrm{mGal}]}. \quad (2)$$

We choose arbitrary point in the western part of Egyptian desert (from Fig. 3a or b), which might indicate a settlement at coast/beach of that hypothetical paleolake. We read the difference Δg between this point and the largest negative anomaly nearly or at the closest minimum of Δg. We get for example Δg = 50–100 mGal, which corresponds to $\Delta h \approx$ 200–400 m. This would be the maximum depth of that paleolake assuming that the topographic depression corresponding to the negative gravity anomaly would be fully filled by water. In the real word, we may expect depths of order of tens of meters and in the case of a canyon (not probable) up to a few hundred meters.

The virtual deformations (Fig. 3d) fully support findings by Δg and T_{zz}. As expected, the compression is observed inside the paleolake and is elongated in the south-north direction. We can see a compression also at some parts of the Nile river, at Fayum, in delta of Nile, south of Kharga, along Dakhla or in the Red sea.

The strike angles (Fig. 3e) show large areas with combed vectors, e.g., in the Red sea, in the whole delta of Nile, a large land west of it, in Siwa area, but also in a part of GSS from Siwa to Gilf Kebir. The places with the combed strike angles clearly correlate with ancient sites (black dots and the cross). From other our investigations (Klokočník et al., 2017a; Klokočník and Kostelecký, 2015 and new work in progress) we know that such areas correlate with deposits of oil or gas or shale gas or (ground)water. In the case of GSS one would also expect underground water/aquifers under a thick sand layer; this might be another very interesting and important finding and application of our methodology for Egypt.

Now to the extent and shape of possible paleolakes. We try to estimate the area covered by the lakes some 8.5–5.3 ky BP in the west Egypt, west of longitude about 30°. We work with dots in Fig. 2c. They are on various contour lines with positive as well as negative values of Δg. If the dots on Fig. 3 a-e are correctly located and if the assumption that the settlements were built mostly near shores is also correct, then we can follow the relevant contour line(s) and depict probable extent and shape of the paleolake or paleolakes. What we may find we should verify by the other gravity aspects. Also we can suggest not yet discovered settlements, now archaeological sites along those shores (probably from the interval 7.0–5.3 ky BC). Of course, the lakes were not stable and forthcoming desiccation led to water level decreasing, which might be irregular process; some settlements disappeared, some may be moved down to a new shore. According to Gehlen et al. (2002) the paleolakes level however might be stable for a long time, up to 3000 years. However, they also claim that the GSS area was relatively arid permanently, thus not too suitable for a lake.

The result of our test is shown in Fig. 4 for Δg with contour lines in 20 mGal interval and with added water level of maximum extent of hypothetical paleolakes. Not all topographic depression means a presence of a lake or rivers; there might be a river or nothing; effect of erosion can be also accounted for. This is our explanation why one dot in Fig. 3c of Kuper and Kroepelin (2006) fits to a bottom of negative Δg.

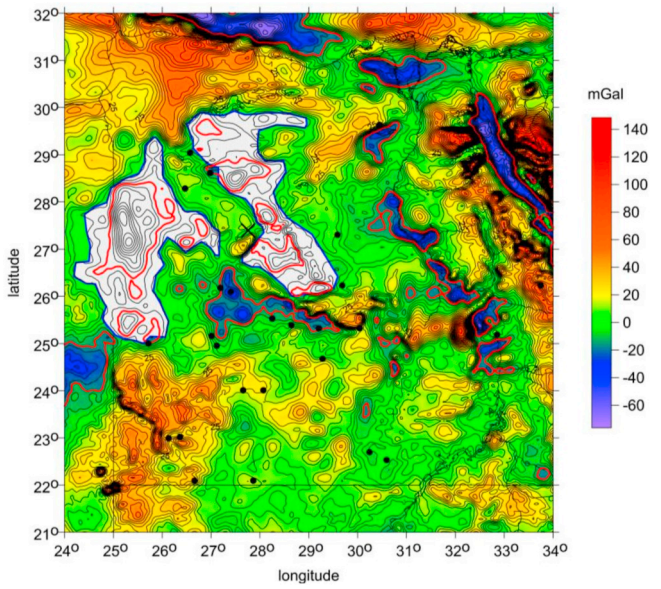

Fig. 4. Boundaries of hypothetical lacustrine depressions in west Egypt, namely below the Great Sand Sea (GSS), according to the gravity disturbances computed from EIGEN 6C4, confirmed by other gravity aspects. Red contours are for −15 mGal, an alternative to blue maximalist paleolakes boundaries; one paleolake breaks up to a few parts. (For interpretation of the references to colour in this figure legend, the reader is referred to the Web version of this article.)

This happened only once from 21 cases.

Can we interpret the large negative anomaly and negative *vd* in GSS by another way? Following Jimenez-Martinez et al. (2015), there might be a river system in the area covering partly the GSS instead of any lake (their Fig. 10), but it is hardly distinguishable whether a lake (or lakes) or a river system by our gravity aspects. What remains in any case is a strong indication of water-filled depression.

5. Repeated dynamics of Sahara lake basins?

Note first about Geological Atlas of Africa (Schlütter, 2006) with an overview of geology of African countries including Egypt (Fig. 68, p. 89) and main rift trends of the whole continent (Fig. 9, p. 23) where the basic geological features including the geodynamic setting are clearly exhibited.

In our previous research we tried to determine the extent of some lake basins distributed in Chad area and former valleys of large rivers namely Paleonile (Klokočník et al., 2017a). The geophysical/gravimetric signal of these basins is strong suggesting the thickness of sedimentary infills in at least first hundred meters as it was proven by drilling in contemporary Nile valley, Fayum Basin and elsewhere especially in the places along the Lower Nile valley flooded by Miocene sea (Said, 1990, 1993, see Fig. 3a and b).

The intensive gravitational anomalies such as in Silica region south of Siwa in Egypt display the existence of large lake basins that must be in the majority cases older than Quaternary, because the gravity signal corresponds to Red Sea rifting zone.

The belt of contemporary oases in Egyptian Western Desert is probably established on the relicts of former large river valley, that was during Oligocene-Upper Miocene (approx. 30-10 My) dissected and partially uplifted by Neoid Cenozoic movements. Oases are found mostly in places that are located 100–200 m under the average level of flat Saharan relief in places where they intersect the deep water table or in some other cases ascending, often hydrothermal springs.

We propose that the intensive aeolian exhumation took place not only in former river valleys but in lacustrine basins as well because they were filled by almost similar type of softer erodible sediments such as sands and clays, while harder Nubian sandstone can be found on the surrounding edges and paleoshores. The cycles of aeolian down cutting probably many times alternated with phases of aeolian accumulation due to the episodes of weaker and stronger winds during warm-cold transitions (Hoelzmann et al., 2004; Burke and Gunnel, 2008; Embabi, 2004).

Therefore, we tend to look at Saharan landscapes as characteristic African etchplain on which during humid phases very large but mostly shallow mostly intermittent lakes existed encircled by a riverine systems. While the ground penetrating radar discovers numerous but mostly shallow Quaternary wadis – so called radar rivers – the massive changes of gravitational field indicate relicts of Tertiary lake basins and valleys of comparable size as present Nile or Lake Chad (McHugh et al., 1988). Thus, the anomalies discovered by GOCE and other data indicate the extent of “Miocene” lakes that due to the preferential wind erosion formed the basis even for large Holocene lakes that were later with the dessication of Sahara subdivided into a number of small lake and/or marsh basins. Maybe several phases of Neolithic occupation can be found – the older ones concentrated on the banks of larger lake and younger ones disseminated around shores of younger, much smaller water bodies. The geophysical anomaly of Silica region represents one of the few most striking gravity signals of the whole Egypt and may thus delineate an important focal point for Miocene as well Quaternary geology and palaeontology.

6. Origin of Libyan Desert glass reconsidered

During the late 90ties and in a few years after year 2000 several illegal expeditions of mineral collectors took place to Silica region (geodetic latitude = $25^0$15‘–$25^0$30‘N, longitude ~ $25^0$30’E) to gather Libyan Desert glass (LDG) that could be sold at international markets for a prize about 1€ per gram and up to 200 kg of glass could be collected in a single day. These expeditions were organised by Bedouins from Libya. We met Libyans south od Siwa so we are aware that the area was sometimes visited from the area beyond Egyptian frontier.

One of the authors of this article encountered in Cairo anonymous German collector, a well educated geologist, who claimed not only to find a number of silica glass artefacts but a thin vein of silica glass about 3 m long as well. We are well aware of the “oriental legends” resembling Victorian fairy tales, we heard this sort of stories fairly often, but let's look if there exists any geophysical evidence for the possibility that impact crater of LDG could be found approximately under the area where the glass now redistributed by younger rivers can be found.

Fig. 5a–d shows the area at El-Obeyid cave at Faráfra oasis (geodet. latitude 27°23.745′N, longitude 27°45.469′E), typical flat terrain with Early Holocene marshes and shallow lakes; the central part of LDG glass area with a few glass fragments, and a relatively common concentration of small angular glass fragments.

We cannot neither approve or reject the hypothesis. The gravitational record of the Silica lake anomaly proves deep almost circular anomaly/anomalies that indicate any type of a basin regardless its origin (Fig. 3 a-c, Fig. 6). The former Eocene-Miocene impact crater – if it has existed at this place – must has been denuded a long ago, so only the root zone of former depression, later probably filled with the water and transformed into a lake, may be preserved. However, we believe that there exists a probability that the impact crater may be discovered in the Silica region approximately under the occurrences of LDG, transported to the shores of the lake by local rivers. It can be too small to be firmly confirmed by the recent gravity data with resolution ~10 km on the ground.

The map of the virtual deformations *vd* (Fig. 3d) manifest other large configuration – a radial geological structure with the centre northwest of Siwa (see the lines in Fig. 3d). The *vd* values represent a complex mathematical model (see Sect. 2, more in Kalvoda et al., 2013 or Klokočník et al., 2017b). From the geological point of view, *vd* appear

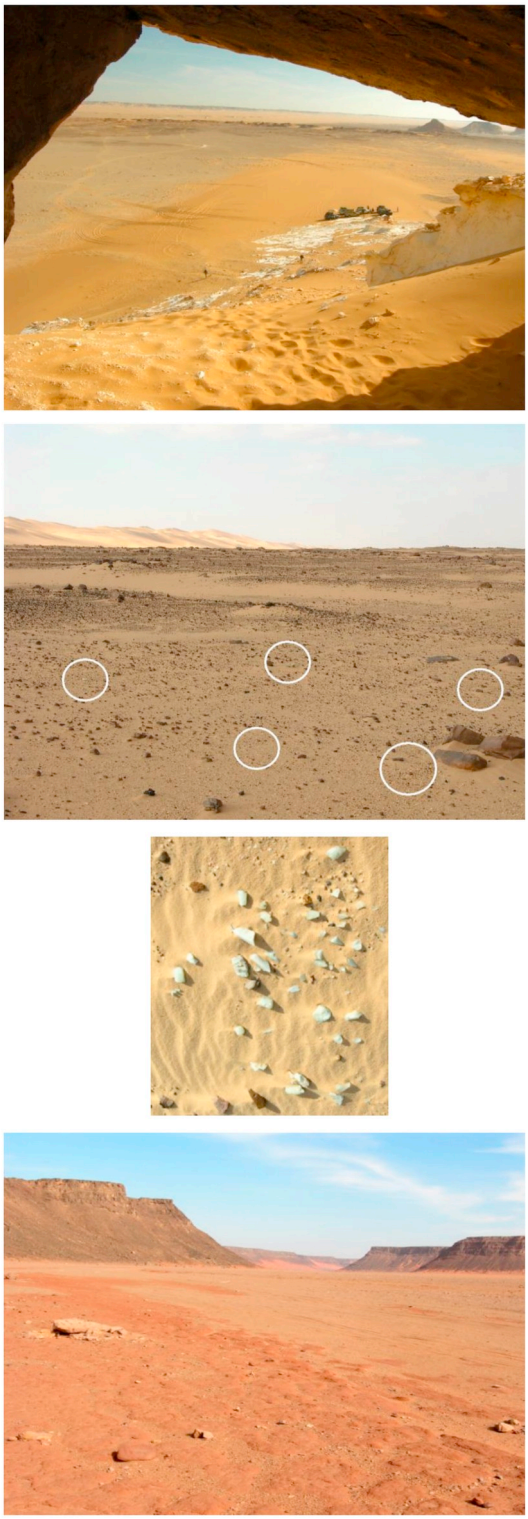

Fig. 5. a The view from El-Obeid cave towards the flat terrain with Early Holocene marshes and shallow lakes. The geographic position of this cave is marked by crossing x in the previous figures. © V. Cílek 2008. **b** The central part of Libyan Desert glass (LDG) area. The circles point to glass fragments on the desert surface. © V. Cílek 2008.**c** The LDG area, zoom of Fig. 5b; example of the glass fragments. © V. Cílek 2008. **d** The large valleys of Gilf Kebir rivers resembling Central Nile Valley abruptly end at the contact with flat plains where their continuation may be in some cases deduced from the gravity signal. © V. Cílek 2008.

in places where some geological activity like dilatations or compressions of plates or extension structures of orogeny took place – these processes and their geological significance can be demonstrated elsewhere, e.g., in the northern part of Red Sea or in Alpine foreland basins. The detected radial structure seems to be longer than most of the usual volcanic radial structures associated with subsidence calderas or alike features, but without geological evidence any explanation (for example their relationship to an impact structure) is highly hypothetic one. We prefer the explanation that these radial structure represents secondary zones of rifting as indicated, e.g., in Schlütter's map of main rift trends (2006, Fig. 9, p. 23).

Fig. 6 shows two profiles; their location was shown by blue curve in Fig. 1a. One profile is based on the present topography derived from ETOPO 1 (Fig. 1a), another on the gravity disturbances from EIGEN 6C4 (Fig. 3a and b). The goal of these graphs is to demonstrate possible location of the paleolake(s) under the sand, in an accord with a possible lake shape and boundaries estimated in Fig. 4, and also possible location of the hypothetical impact crater, the feasible source of LDG. This impact structure might be well a part of the paleolake(s), regardless its age.

We know that about the position of the "source impact crater" for LDG there are various speculations, for example that it is the Kebira crater (latitude = $24^0$40'N, longitude = $24^0$58'E) or that the crater does not exist (the impactor might be a comet and explosion would take place above the surface) or that the crater was denudated by subsequent external and internal forces and nothing after that event remained obvious (Mizera et al., 2017).

It is important to note that the impact origin of Kebira crater on border of Libya and Egypt or nearby Gilf Kebir crater field (latitudes = $23^0$14'– $23^0$32'N, longitudes = $23^0$17'– $27^0$27'E) is not confirmed so the other possibilities of the LDG original site including Silica region are still opened for further research. We save many references by citing excellent review about impact structures in Africa by Reinold and Koeberl (2014, mainly pp. 133–135 and 155–156).

7. Conclusion

We provide a new look at Eastern Sahara including Great Sand Sea (GSS) with the gravity aspects (like the gravity disturbances, second radial derivatives, strike angles and virtual deformations) computed from the global gravity field model EIGEN 6C4 (Fig. 3 a-e, 6). The ETOPO 1 satellite topography model serves as a subsidiary data file (Figs. 1a and 6). We correlate the features found from the gravity data with the locations of the Holocene occupations in the Eastern Sahara since the onset of humid conditions about 11 ky BC till the intensive desiccation approx. four thousand years ago (Fig. 2 a-d); the correlation is very good (Fig. 3 a-c). Based on this finding, we derive estimates of a possible location, extent and shape of the putative paleolake(s), assuming that the archaeological sites were situated mostly at more or less stable lake borders or at rivers (Fig. 4). This is our main result (Figs. 4 and 6). We speculate that while the archaeological sites given in Kuper and Kroepelin (2006) are on "open air", hypothetical sites in GSS can be hidden under a thick layers of sand (Fig. 6) and might be discovered in future; it might be with the aid of Fig. 4.

We also we reconsider the origin of Libyan Desert glass (LDG) in GSS and support the hypothesis about an older impact structure repeatedly filled by water, a part of the possible paleolake(s) or river system or a combination of both located close to the contemporary finds of the LDG (Fig. 5a–c, 6). In the case of GSS, we may also expect ground water under thick sand layers; this might be another separate and important result of our methodology for Egypt, so this topic should be studied further on.

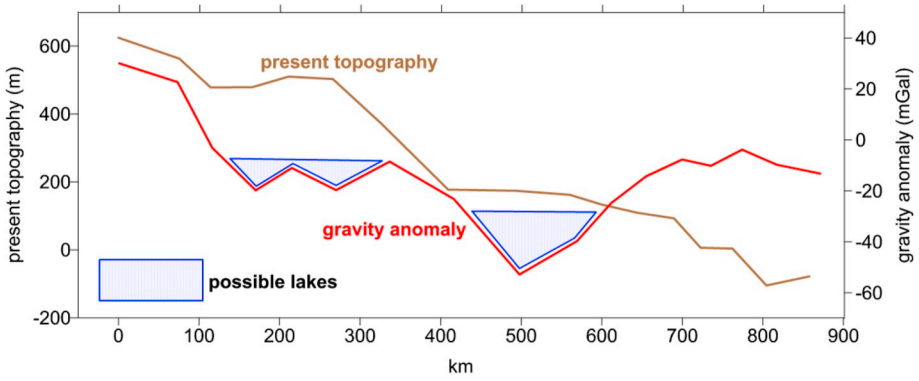

Fig. 6. The profiles of present topography from ETOPO 1 model and from gravity disturbances Δg derived from EIGEN 6C4 along the trace shown in Fig. 1a from south to north in western Egypt indicating possible location of the paleolake(s) including also the Eocene-Miocene impact crater, a putative source of LDG. To transform the values of Δg to the height differences Δh, use eq (2). The distance "zero" is at the south end of blue curve in Fig. 1a and is counted along this curve to north. Roughly it holds that 100 km = 1^0. (For interpretation of the references to colour in this figure legend, the reader is referred to the Web version of this article.)

Declaration of competing interest

The authors declare that they have no known competing financial interests or personal relationships that could have appeared to influence the work reported in this paper.

Acknowledgments

This work has been prepared in the frame of project RVO #67985815 (Czech Academy of Sciences, Czech Republic), partly supported also by the project LO1506 (PUNTIS) from the Ministry of Education of the Czech Republic. We thank B. Bucha for the computations of the gravity aspects with EIGEN 6C4. We thank also M. Verner and L. Varadzinová (Czech Institute of Egyptology, Charles University, Faculty of Arts, Praha, Czech Republic) for consultations and literature from their specialisation and J. Mizera (Nuclear Physics Institute of the Czech Academy of Sciences, Řež, Czech Republic) for consultations and literature from his specialisation.

References

Abd-Elmotaal, H., Seitz, K., Kühtreiber, N., Heck, B., 2018. AFRGDB_V2.0: the gravity database for the geoid determination in Africa. In: The International Association of Geodesy Symposia. Springer, Berlin, Heidelberg, pp. 1–10. https://doi.org/10.1007/1345_2018_29.

Amante, C., Eakins, B.W., 2009. ETOPO1, 1 arc-minute global relief model: procedures, data sources and analysis. NOAA Techn. Memo. NESDIS NGDC 24https://doi.org/10.7289/V5C8276M. (National Geophysical Data Center).

Beiki, M., Pedersen, L.B., 2010. Eigenvector analysis of gravity gradient tensor to locate geologic bodies. Geophysics 75, 137–149. https://doi.org/10.1190/1.3484098.

Bucha, B., Janák, J., 2013. A MATLAB-based graphical user interface program for computing functionals of the geopotential up to ultra-high degrees and orders. Comput. Geosci. 56, 186–196. https://doi.org/10.1016/j.cageo.2013.03.012.

Burke, K., Gunnel, Y., 2008. The African erosion surface: a Continental-Scale Synthesis of Geomorphology, tectonics, and environmental change over the past 180 Million Years. Memoirs 201, 37–44 (Boulder, Colorado).

Burroughs, W.J., 2005. Climate Change in Prehistory. Cambridge Univ. Press ISBN-10 0-521-82409-5.

Coulthard, T.J., Ramirez, Jorge A., Barton, N., Rogeson, M., Brücher, T., 2013. Were rivers flowing across the Sahara during the last interglacial? Implications for human migration through Africa. PloS One. https://doi.org/10.1371/journal.pone.0074834.

Embabi, N.S., 2004. *The Geomorphology of Egypt. Landform evolution.* Vol. I, the Nile Valley and the Western Desert. The Egyptian Geographical Society, Cairo, pp. 32–70.

Eppelbaum, L.V., 2017. From Micro- to satellite gravity: Understanding the Earth. American Journal of Geographical Research and Reviews 1, 3. https://doi.org/10.28933/ajgrr-2017-12-0501. eSciPub.

Eppelbaum, L.V., Katz, Y., Klokočník, J., Kostelecký, J., Ben-Avraham, Z., Zheludev, V., 2017. Tectonic Insights into the Arabian-African region inferred from a comprehensive Examination of satellite gravity big data. Global Planet. Change 159, 1–24. https://doi.org/10.1016/j.gloplacha.2017.10.011. https://www.researchgate.net/publication/320625566.

El-Baz, Farouk, 1998. Aeolian deposits and palaeo-rivers of the eastern Sahara. Significance to archaeology and groundwater exploration, *Sahara* 10, 55–66.

Förste, Ch, Bruinsma, S., Abrykosov, O., Lemoine, J.-M., et al., 2014. The latest combined global gravity field model including GOCE data up to degree and order 2190 of GFZ Potsdam and GRGS Toulouse (EIGEN 6C4). 5th GOCE user workshop. Population (Paris) 25–28 Nov.

Gehlen, B., Kindermann, K., Linstädter, J., Riemer, H., 2002. The Holocene occupation of the eastern Sahara: regional Chronologies and Supra-regional Developments in four areas of the Absolute desert. In: Jennerstraße 8 (Ed.), Tides of the Desert – Gezeiten der Wüste. Contributions to the Archaeology and Environmental History of Africa in Honour of Rudolph Kuper. *Africa Praehistorica* 14. Köln (Heinrich-Barth-Institut), pp. 85–116.

Hoelzmann, P., et al., 2004. Palaeoenvironmental changes in the arid and sub arid belt (Sahara-Sahel-Arabian Peninsula) from 150 kyr to present. In: Battarbee, R.W. (Ed.), Past Climate Variability through Europe and Africa. Kluwer Acad. Publ., Dordrecht, pp. 219–256. https://doi.org/10.1007/978-1-4020-2121-3_12.

Jimenez-Martinez, N., Raminez, M., Diaz-Hernandez, R., Rodriguez-Gomez, G., 2015. Fluvial transport model from spatial distribution analysis of Libyan Deser Glass mass on the Great Sand Sea (Southwest Egypt): Clues to primary glass distribution. Geosciences 5, 95–116. https://doi.org/10.3390/geosciences5020095.

Kalvoda, J., Klokočník, J., Kostelecký, J., Bezděk, A., 2013. Mass distribution of Earth landforms determined by aspects of the geopotential as computed from the global gravity field model EGM 2008. Acta Univ. Carolinae, Geographica XLVIII (2) (Prague).

Klokočník, J., Kostelecký, J., 2015. Gravity signal at Ghawar, Saudi Arabia, from the global gravitational field model EGM 2008 and similarities around. Arab. J. Geosciences 8, 3515–3522. https://doi.org/10.1007/s12517-014-1491-y. ISSN 1866–7511, (Springer-Verlag).

Klokočník, J., Kalvoda, J., Kostelecký, J., Eppelbaum, L.V., Bezděk, A., 2014. Gravity Disturbances, Marussi Tensor, Invariants and Other Functions of the Geopotential Represented by EGM 2008, ESA Living Planet Symp. 9-13 Sept. 2013, Edinburgh, Scotland. Publ. In: August 2014: J Earth Sci. Res 2. pp. 88–101.

Klokočník, J., Kostelecký, J., Bezděk, A., 2016. On feasibility to detect volcanoes hidden under ice of Antarctica via their "gravitational signal. Annals of Geophys 59, 5. https://doi.org/10.4401/ag-7102. S0539.

Klokočník, J., Kostelecký, J., Cílek, V., Bezděk, A., Pešek, I., 2017a. A support for the existence of paleolakes and paleorivers buried under Saharan sand by means of "gravitational signal" from EIGEN 6C4. *Arab. J. Geosciences,* on-line. https://doi.org/10.1007/s12517-017-2962-8.

Klokočník, J., Kostelecký, J., Bezděk, A., 2017b. Gravitational Atlas of Antarctica. Series Springer Geophysics; Springer Nature (Book). vol. 113978-3-319-56639-9.

Klokočník, J., Kostelecký, J., Bezděk, A., 2018. Gravito- topographic signal of the Lake Vostok area, Antarctica, with the most recent data. Polar Science. https://doi.org/10.1016/j.polar.2018.05.002.

Kuper, R., Kroepelin, S., 2006. Climate-controlled Holocene occupation in the Sahara: Motor of Africa's evolution. Science 313, 803–807. www.sciencemag.org.

McHugh, W., McCauley, J.F., Haynes, V., Breed, C.S., Schaber, G.G., 1988. Paleorivers and Geoarchaeology in the southern Egyptian Sahara. Geoarcheology 3 (1), 1–40.

Mizera, J., Řanda, Z., Krausová, I., 2017. Neutron and photon activation analyses in geochemical characterization of Libyan Desert Glass. J. Radioanal. Nucl. Chem. 311, 1465–1471. https://doi.org/10.1007/s10967-016-5094-9.

Pavlis, N.K., Holmes, S.A., Kenyon, S.C., Factor, J.K., 2012. The development and evaluation of the Earth gravitational model 2008 (EGM2008). J. Geophys. Res. 17, B04406. https://doi.org/10.1029/2011JB008916. 2012; original conf. pres. in 2008.

Pedersen, B.D., Rasmussen, T.M., 1990. The gradient tensor of potential field anomalies: some implications on data collection and data processing of maps. Geophysics 55, 1558–1566.

Pick, M., Pícha, J., Vyskočil, V., 1973. *Úvod Ke Studiu Tíhového Pole Země* (In Czech, *Introduction to Study of the Gravity Field of the Earth*). Academia, Praha.

Reinold, W.U., Koeberl, Ch, 2014. Impact structures in Africa: a review. J. Afr. Earth Sci. 93, 57–175. https://doi.org/10.1016/j.jafrearsci.2014.01.008.

Saad, A.H., 2006. In: Van Nieuwenhuise, B. (Ed.), Understanding Gravity Gradients - a Tutorial, the Meter Reader, pp. 941–949 August issue, The Leading Edge.

Said, R., 1990. In: Balkema, A.A. (Ed.), The Geology of Egypt, pp. 720 (Rotterdam).

Said, R., 1993. The River Nile. Geology, Hydrology and Utilization. Pergamon Press, pp. 320.

Schlűtter, T., 2006. Geological Atlas of Africa. Springer-Verlag, pp. 218–220.

Sobh, M., Mansi, A.H., Ebbing, J., Campbel, S., 2019. Regional gravity field model of Egypt based on the satellite and ground-based data. Pure Appl. Geophys. https://doi.org/10.1007/s00024-018-1982-y.